EXEPRIMENTAL TESTING OF A TREMOR COMPENSATION SYSTEM WITH BIMORPH PIEZOCERAMIC ACTUATORS USING OPTICAL METHODS

Dragos Ovezea[1], Romulus M. Mihai[1,3], Cristinel Ilie[1], Adrian Nedelcu[1], Nicolae Tanase[1,2], Marius Popa[1,2], Mihai Guțu[1]
[1]National Institute for Research and Development in Electrical Engineering ICPE-CA,
Splaiul Unirii no. 313, 030138, District 3, Bucharest, Romania
[2]Polytechnic University of Bucharest - UPB – Doctoral School of Electrical Engineering
Splaiul Independenței nr. 313, Sector 6, Bucharest, Romania
[3]Valahia University from Târgoviște, Dâmbovița County, 130004, Romania
E-mail: dragos.ovezea@icpe-ca.ro, romulus.mihai@icpe-ca.ro, cristinel.ilie@icpe-ca.ro , adrian.nedelcu@icpe-ca.ro, nicolae.tanase@icpe-ca.ro, marius.popa@icpe-ca.ro , mihai.gutu@icpe-ca.ro

Abstract – The purpose of this paper is to present a new stand developed for exeprimental testing of a tremor compensation system with bimorph piezoceramic actuators using optical methods. The characterization of the bimorphic actuators was performed by plotting the response curve, for displacements between 0 and 150 V. A new method for determining the response curve has also been developed, using optical image capture and processing. Comparing the results obtained using the optical method with those obtained by manual reading the measurements, it was found that similar results were obtained, relative to the type and maximum deflection of the tested actuators, which validates the new optical developed method by ICPE-CA.

Keywords: Tremor compensation, Biomorphic piezoelectric micro actuators, Optical measurements, LASER system.

1. Introduction

Current microsurgical systems are based on the surgeon's ability to make very fine movements with a very low level of vibration at the end point. This goal requires highly competent staff and limits the duration of work, limits the types of microsurgical procedures and limits the quality of those performed. Therefore, the effective reduction of involuntary or unwanted movement in microsurgery (surgeon tremor) would not only improve the accuracy of existing procedures, but could pave the way for new types of procedures [1-3].

Robot-assisted surgery is used in a wide variety of surgical applications because it provides fine handling and very good precision, ensuring the dexterity needed for matte complexity operations. Despite the commercial success of robotic platforms, the practical use in microsurgery is still deficient due to the lack of reaction from the patient, a reaction necessary to maintain a high level of accuracy at submillimeter displacements [1-3].

Microsurgical techniques are used by several specialties, such as: general surgery, ophthalmology, orthopedic surgery, gynecological surgery, otorhinolaryngology, neurosurgery, oral and maxillofacial surgery, plastic surgery and pediatric surgery.

Surgeons and people in general have intrinsic limitations on the accuracy of manual positioning. These limitations are the consequences of small involuntary movements that are inherent in normal hand movement. These limitations are the consequences of small involuntary movements that are inherent in normal hand movement. This inaccuracy prevents the correct handling of micromanipulating tasks, not being able to distinguish between intentional movement and involuntary movements of the same order of magnitude. From a technical point of view, it is a low signal-to-noise ratio.

Considering the above, it is necessary to develop a precision displacement system for microsurgical instruments, so that, following the measurements, make it possible to model the tremor and error for the development of algorithms for estimating errors and quantitative testing of the obtained results [1-3].

Micromanipulation is a difficult task even for surgeons specializing in microsurgery. Although they are known for their stable hands, they have physiological (involuntary) tremor, which makes certain microsurgical procedures difficult or even impossible [4]. Robot-assisted micromanipulation is

a promising solution to these problems because it has offered a variety of advantages over conventional techniques, applied in biomedical fields [5-7].

For instance, the robotic platforms allow fine, precise, and highly dexterous handling during surgery by tremor filtering and motion scaling [8 -10]. Furthermore, the secondary tasks can be automated, reducing the cognitive load of repetitive procedures and improving accuracy [11].

A closer approach to conventional ones [10, 11] uses the tremor compensation implemented in a fully portable microsurgical instrument. The instrument is designed to determine its own movement and to distinguish between intentional and erroneous movement, so as to deflect its tip to cancel the unwanted component in real time.

The expansion of medical applications in the field of microsurgery is a natural development. Moreover, the development of systems to ensure the stability of working tools with the help of real-time vibration compensation can be used also in other applications where special precision and stability of the instrument at random vibrations is required. This tremor is approximately sinusoidal with a typical amplitude of 50 μm (peak to peak) and a frequency between 8-12 Hz [3].

2. Constructive Solutions for LASER Beam Vibration Compensation Systems for Microsurgery

AI. Constructive solution with displacement amplified piezoelectric actuators using a Stewart platform

The first built system uses piezoelectric microactuators with displacement amplification, according to Fig. 1 and Fig. 2 which, by means of a compliant mechanism, acts on the LASER collimator with optical fiber, rigidly fixed to it.

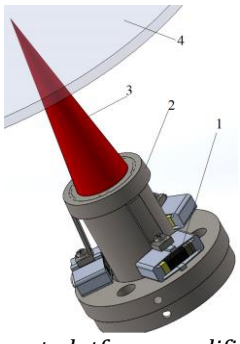

Figure 1: Stewart platform amplification system assembly: 1-piezoelectric actuator with displacement amplification; 2-mechanical system with compliant mechanism; 3 - LASER beam; 4 - work surface.

The transmission of the motion from the actuating elements presented above is performed by means of a compliant mechanism which has as starting point the amplifying mechanism presented, as can be seen in Fig. 1.

For this system were used three such piezoceramic actuators, arranged equidistant on a circle at 120^0 (Fig.2).

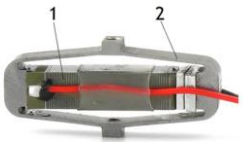

Figure 2: Piezoelectric microactuator: 1- Stack piezoceramic pills; 2- metal frame [12].

AII. Constructive solution with bimorph actuators

Bimorph actuators are a type of piezoelectric actuators made of "soft" PZT materials; they are supplied at low voltages (hundreds of volts instead of kilovolts), and the electromechanical coupling coefficient is d31, which means that the relevant deformation takes place perpendicular to the direction polarization. By a special arrangement of the layers of material, large deformations can be obtained with small clamping forces (hundreds of μm and Newtons).

Figure 3 presents an example of a monomorphic structure 0, functionally similar to a bimetal, made with a PZT layer and a steel layer. Feeding the PZT layer will cause it to bend. Usually, in order to obtain higher deformations and forces, actuators with two piezoelectric layers placed on either side of a common electrode, called "bimorph" structures, are used.

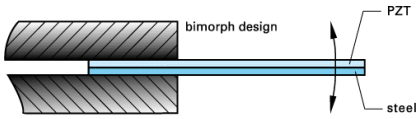

Figure 3: Monomorphic piezoelectric actuator capable of 0 bending.

The constructive solution of the tremor compensation system with bimorph actuators is presented in Fig. 4.

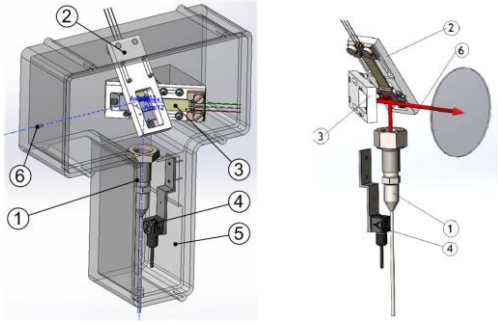

a) *b)*

Figure 4: Constructive solution for vibration compensation system with two orthogonal LASER deflection systems, in two directions [13].

Figure 4 shows the system components of the random motion compensation and can be seen the optical system (1) which projects the LASER beam transmitted by optical fiber, the deflection systems (2) and (3), the space relative orientation sensor and vibration detection (4), all of which are contained in a pistol-like housing (5). The constructive solution developed to compensate for the random movements of the hand, which looks similar to a pistol, has a handle that can be held by the surgeon and the LASER beam can be projected forward, similar to how the gun can launch bullets.

The path of the LASER beam was represented by a dotted line. It can be seen that the directions in which it moves are orthogonal and that there is an exit hole, in the pistol housing (6).

To test the laboratory model for the vibration compensation system, a stand was made containing two orthogonally placed actuators and a LASER that ensures the beam to be deflected controlled.

For the bimorph actuators, the PB4NB2S model was chosen (Fig. 5), produced by ThorLab, with the following technical characteristics:

- working voltage: 0 – 150 V
- displacement from 150 V: ±450 µm ±15%
- Hysteresis: ≤15%
- Free length: 28 mm
- Locking force at 150V: 1,5 N
- Resonant frequency: 270 Hz
- Overall dimensions: 32 x 7,8 x0,8 mm^3.

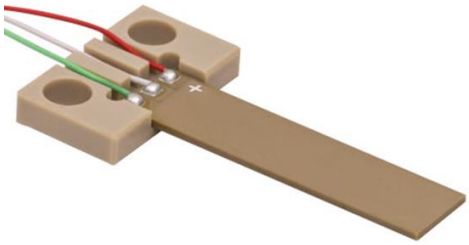

Figure 5: Bimorph piezoelectric actuator, type PB4NB2S [14].

For the constructive solution with bimorph actuators, the solved problems consisted in choosing the type of connection between the bimorphic actuator and the flat mirror that directs the LASER beam.

3. Stand for Characterization of Bimorphic Piezoelectric Actuators and Bidirectional LASER Beam Guidance System

To change the direction of the LASER beam, a stand was made with a simple constructive solution, in which the mirror is fixed by means of an adapter piece or directly, by gluing the mirror on the surface of the actuator.

The testing structure consists of a support on which are made two prisms for mounting the actuators in the required position, Fig. 6. The mirrors are mounted at the free end of the actuator, as far away from the base as possible, so that the LASER beam can be deflected in two perpendicular directions.

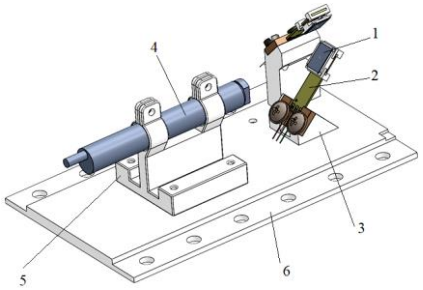

Figure 6: Stand for testing bimorph actuators and bidirectional LASER beam guidance system mechanical structure: 1-mirror; 2-piezoelectric bimorph actuator; 3-hardening support; 4-fiber optic LASER; 5- LASER support; 6- base plate.

The two mounting prisms for the actuators are made so as to form a common body with the base on which they are placed so that to facility their relative positioning and minimize possible mounting errors.

The LASER system is mounted on a separate support. The grip is removable and, if necessary, the laser can be changed

It also allows the installation of a smaller solid state LASER, model LC-LMD-650-03. In Fig. 7 it can be seen an image from the catalog sheet of this device. It was purchased for its small size and light weight, as well as its low emission power, below 1mW, which makes it much safer than other commercially available models. The rated emission power is in class 2 (low risk, no special warnings, but with the recommendation to avoid looking directly at the LASER source).

Laser Module
LC-LMD-650-03

LASER COMPONENTS

Electrical and Optical Characteristics (T_C = 25 °C)

Item	Symbol		Min.	Typ.	Max	Unit	Condition
Wavelength	λ		645	655	660	nm	P_{opt} = < 3 mW
Output power	P_{out}	01	-	0.6	0.9	mW	V_{cc} = 3 V
		03	2.2	-	3.0	mW	V_{cc} = 3 V
Operation current	I_{op}		-	15	25	mA	P_{out} = 3 mW
							V_{cc} = 3 V
Operation voltage	V_{op}		2.5	-	3.3	Volt	
Laser Beam spot size at 10 m	< 10 mm						
Divergence angle	1.1 mrad						
Mean time to failure (MTTF) 3 mW 25 °C	>10000 hrs						

Figure 7: Extract from the catalog sheet of the LASER module LC-LMD-650-03 [15].

The measurement stand consists of the guide structure described above in Fig. 6, a screen on which the LASER beam can be projected, a webcam

for position reading, an actuator power supply system and a control program made on the PC in LabVIEW, Fig. 8.

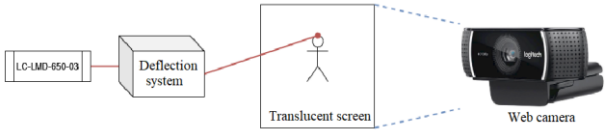

Figure 8: Schematic diagram of the stand for characterizing the bidirectional LASER beam guidance system.

In Fig. 8 it can be seen that the LASER beam is guided by a piezoelectric deflection system and projected on a translucent screen. Behind the screen is a Logitech C922 webcam that allows to record the position of the spotlight relative to a grid printed on the screen, of known size. Based on the camera resolution, grid size and relative position of the light spot relative to the grid, the characteristic of each individual actuator can be obtained in the form of position graphs as a function of the control voltage. These graphs can then be used to compensate for the hysteresis of the actuators (feature linearization) using a feed-forward algorithm based for example on a Preisach model of the actuator.

Knowing the dimensions of the grid and the distance between the screen and the deflection system, the exact angles of variation with the voltage of the system, horizontally and vertically, can be determined. In Fig. 9 it is presented the stand made for testing the bimorph actuators and the bidirectional LASER beam guidance system.

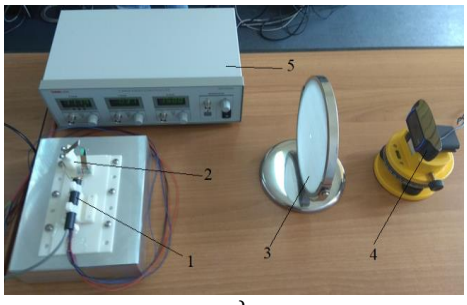

a)

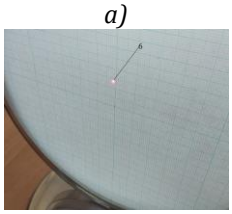

b)

Figure 9: Stand for testing bimorph actuators and bidirectional LASER (piezo deflection system) guidance system. a) overview and b) spot details: 1-LASER; 2-deflection system with piezoelectric actuators; 3-gratulated translucent screen; 4-webcam; 5-voltage generator for piezoelectric actuators; 6-spot laser lights.

The constructive solution in which the bimorph actuators in the version with 3D support for the mirror are replaced with the bimorph actuators in the variant with the adhesion of the mirror on the surface is presented in Fig. 10. For simplification it has been mounted on a modular system.

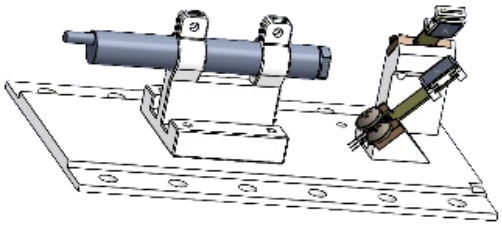

a) mirror fixed with the intermediate 3D part

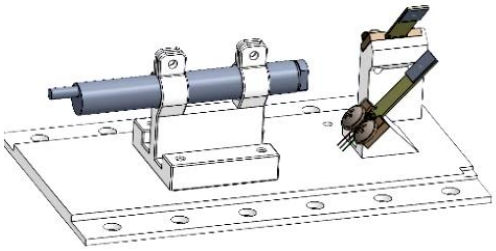

b) glued mirror

Figure 10: The constructive solution of the tremor compensation system in two variants.

4. Characterization of the Bimorph Piezoelectric Actuators and Bidirectional LASER Beam Guidance System

The actuators (Fig. 11) are controlled by means of the excitation voltage, with values between 0 and 150 V. The deflection is determined on a screen located at a known distance from the actuators, in a system of *X-Y* coordinates. Determinations were made on each axis, keeping the power supply to the other actuator at a fixed value of 75 V. Measurements were made manually, by varying the excitation voltage, and for subsequent determinations, automatic motion control programs were used.

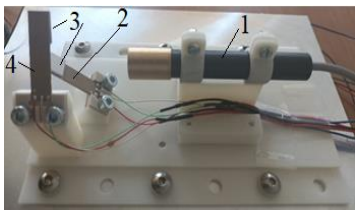

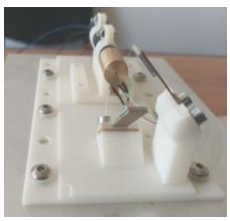

Figure 11: Stand for characterizing the static and dynamic behavior of piezoelectric actuators and the bidirectional laser beam guidance system. Two-way LASER deflection system 1-LASER; 2,4-actuators; 3-mirrors.

For measurements, two constructive solutions were used, one in which the mirrors are attached to the actuator by a 3D support and the second in which the mirror surface is glued directly to the surface of the actuator.

The results are shown in Fig. 12 and Fig. 13, the presence of hysteresis can be observed on both axes (XY), but of relatively low value compared to the total displacement.

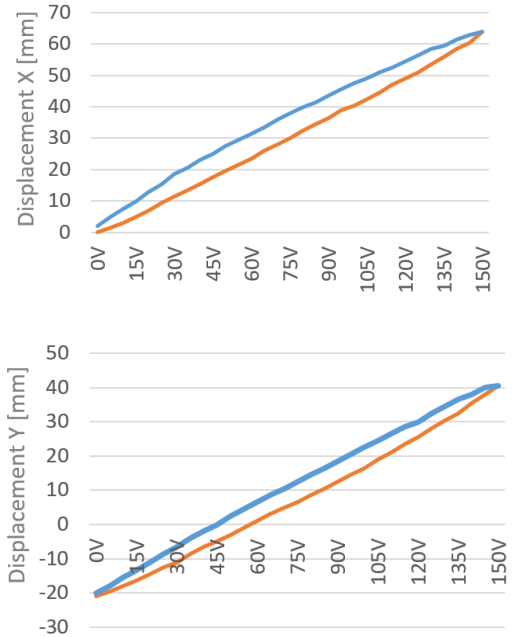

Figure 12: Characterization of the static behavior of piezoelectric actuators, version with 3D support. Displacement in mm, at a distance d = 0.77m.

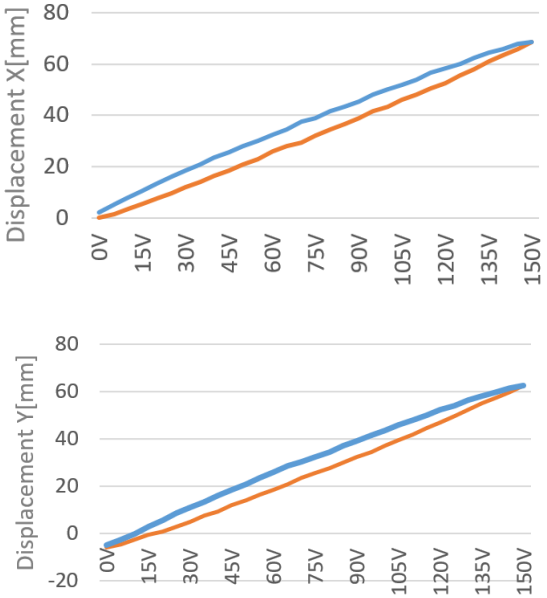

Figure 13: Characterization of the static behavior of piezoelectric actuators, variant with the adhesion of the mirror on the surface. Displacement in mm, at a distance d = 0.80m.

A parasitic displacement in the direction in which we have no variations in the supply voltage was also highlighted, an important parasitic displacement for the version with 3D support and negligible on the axis for the variant with adhesion surface mirrors.

The variant in which the mirror has a common body with the actuator, led to a much more accurate displacement. Its increased rigidity makes the parasitic displacements on the complementary axes smaller in this case. If in the first variant (with 3D suport) we have, according to the measurements performed, a parasitic displacement of 2.5 and 5 mm, respectively, in variant with adhesive mirror we have parasitic displacements of 1.5 and 0.5 mm.

5. Development of the Required Programs for Optical Measurements

In order to determine the XY characteristic of the LASER beam deflection system (Fig. 14) as a subsystem in the vibration compensation system, an optical method had to be found, as the usual equipment generally used to characterize piezoceramic compression actuators (Millimar C1240) [16] has a force of measurement comparable to the locking force of the actuators. Moreover, because the loading force is given by a spring, this force is variable.

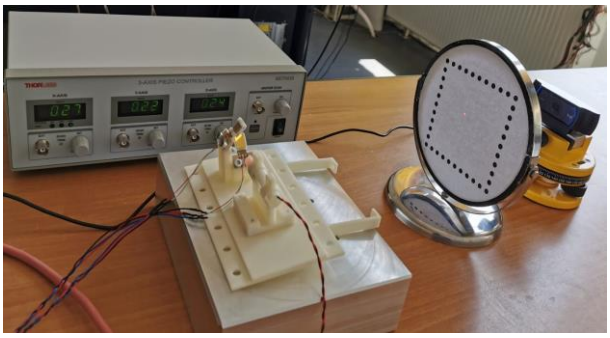

Figure 14: Non-contact method stand.

Thus, a non-contact method was conceived. The basic principle presented in Fig. 14 consists in the projection of the LASER beam on a semi-transparent screen with a grid and the measurement of the position of the spot using a camera. In this case, bimorphic piezoceramic actuators type PB4VB2W with ± 135 μm maximum displacement were used.

There are several problems that have to be tackled.

A) Data acquisition solution

Since the "Vision" module of LabView was unavailable, an alternate method for reliable programmatically acquisition of images was required. Several methods were experimented:

• first the use of a time-lapse software that posted captured images to a HTTP server or to a folder but various errors occurred, some of server response time and others of read-write rights on the files;

• secondly a program called "RobotEyez.exe" [17] was used which allows command line arguments. This is the solution used.

A piece of code was written to call the .exe with specific arguments such as picture resolution and save file format. Because this program initializes the camera every time, acquires the image and then closes, it has a long time to act (~2,7 seconds) but it does not lock the files. Since the program saves the files with the same name, the erasure of the previous file is required. In order to protect the drives from repeated writes which would degrade the location, a RAM-drive was generated and all saving and the related read-write operations take place in RAM memory.

The image capture VI's connections can be seen in Fig. 15.

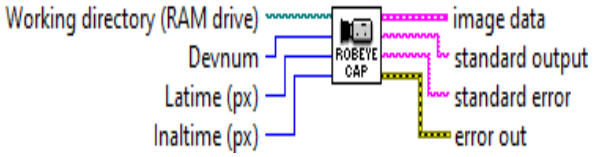

Figure 15: Input – output wiring of the "RobotEyez.vi"

The VI requires the path to the RAM drive, the numerical index of the camera (in case there are more than one), the width and height of the picture. Image data in LabVIEW format is available as well as possible error indicators (Fig. 16).

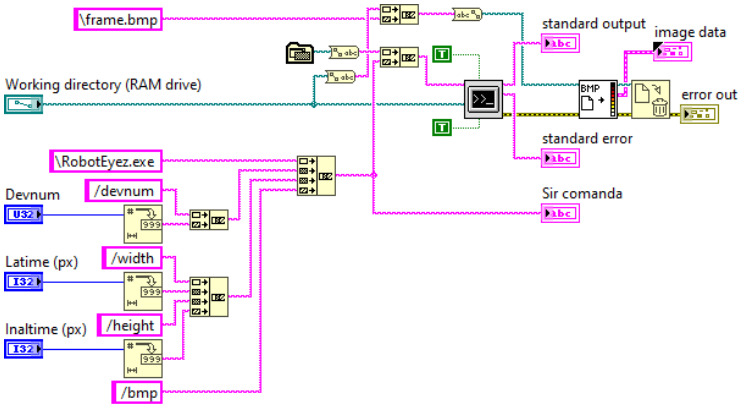

Figure 16: "RobotEyez.vi" code

The files written on the RAM drive are BMP, are read and then deleted. This allows for good use of memory space. The image data is exported and then the file is deleted.

Based on this wrapper VI, a few programs were written. One for actual image acquisition and one for image processing and raw numerical data extraction.

A combined program could have been written but this way seemed better since it allows for other sources of images too. Also, since both the image acquisition and processing are slow, another separate program for numerical data interpretation will have to be written.

The data acquisition program's interface can be seen in Fig. 17.

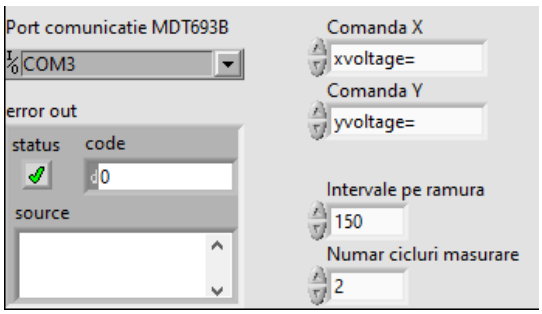

Figure 17: Data acquisition program interface

The path to the folder were the image data will be saved can be selected, the COM number of the MDT693B (voltage amplifier for driving the actuators) and specifications for the voltage applied such as number of intervals on the rising and descending pathways, and the number of cycles to be run. For a 1 V resolution, 150 intervals ensure about 300 points per cycle.

The code of the VI can be seen in Fig. 18.

The captured files are stored in a folder as PNG and are named automatically.

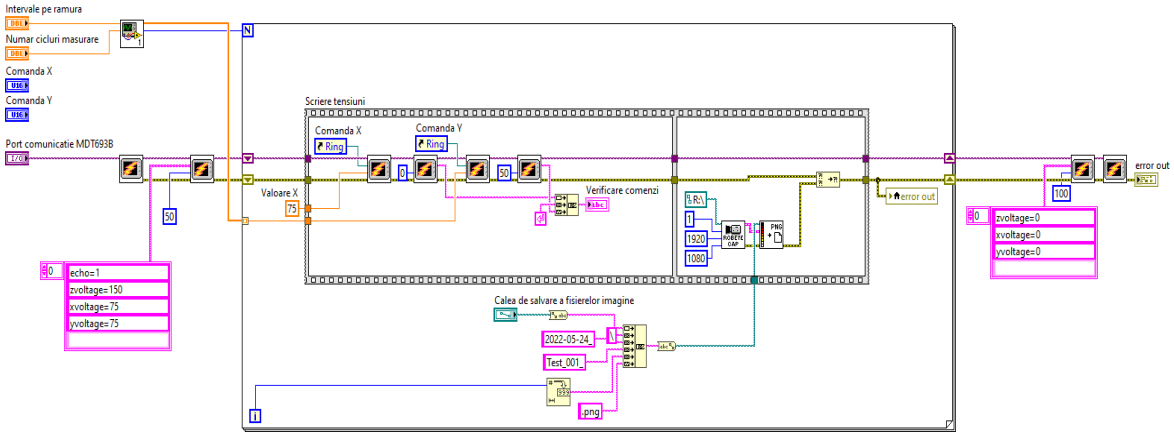

Figure 18: Code of the data acquisition program

B) Image processing solution

A number of 601 color PNG files were acquired (1.5GB) and a selection from one of the pictures is presented in Fig. 19. The red dot of the LASER is visible, and also the black dots of the grid. It can be easily observed that the grid is slightly rotated.

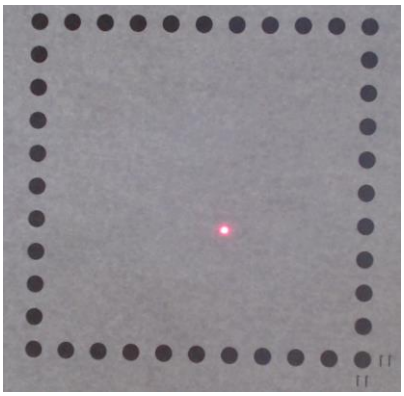

Figure 19: Selection from a captured image with dot grid and LASER spot visible

The image processing software interface can be seen in Fig. 20.

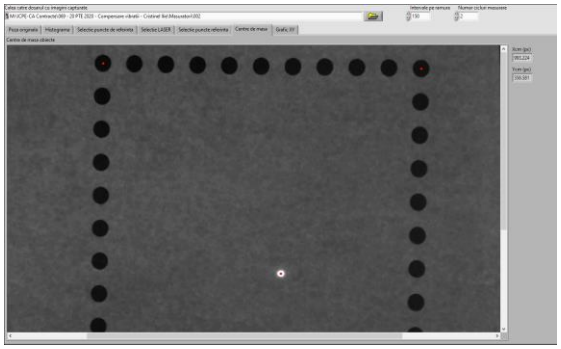

Figure 20: The interface of the image processing program

The program allows the selection of a folder containing the captured images and loads them sequentially. Some of the parameters are selected at the time of the loading of the first image: the image data is separated in three planes of color (RGB) and a brightness plane (L); a histogram (Fig. 21) of these four planes is presented to the user and the threshold levels for LASER beam spot and the black grid spots are set.

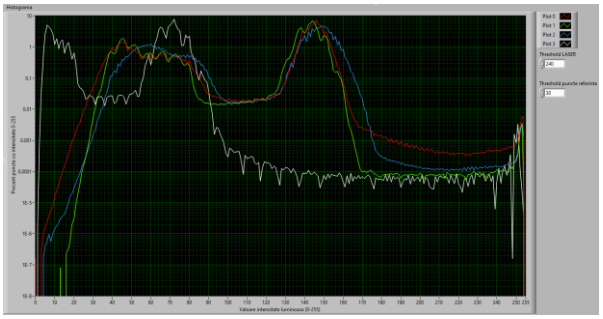

Figure 21: RGBL planes histogram

In order to continue, the program requires the user for a one-time selection of the areas of the picture in which the four corners of the grid are found. These areas will be used in order to restrict calculation of the center of the graphical objects (the black spots in the corners Fig. 22).

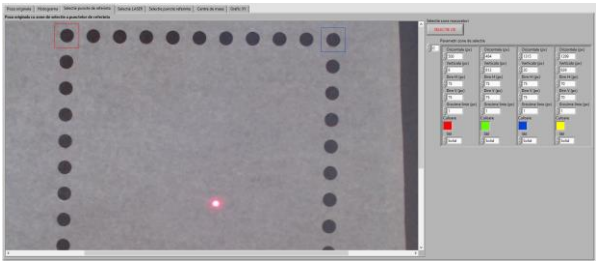

Figure 22: Selection of the areas in which the corner spots are found on the grid

After confirming the selection, the program runs automatically until all the images are processed.

Several graphical representations are offered, for the areas representing the LASER spot and the corner grid locations. Another graphical representation overlaps the original image (the brightness plane) and several red spots corresponding to the center of mass of the objects in the areas of interest (Fig. 23).

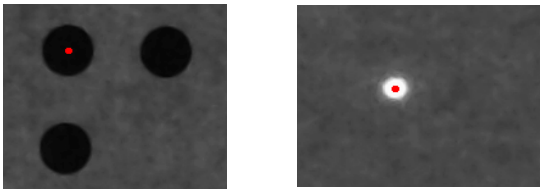

a) center of mass for black grid marker *b) center of mass for LASER spot*

Figure 23: Selection of graphical data representation with red dots placed at the coordinates of the center of mass

During the processing, a XY graph is constantly updated with the location of the actuator's vertical position versus the voltage supplied to the actuator. Thus, a characteristic curve (for piezoelectric actuators) is obtained (Fig. 24).

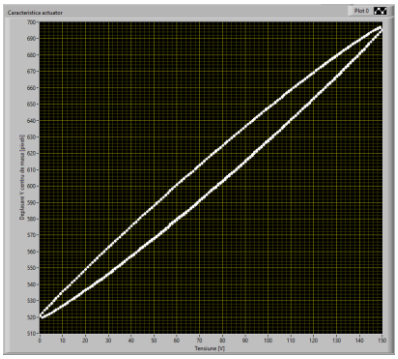

Figure 24: Vertical actuator characteristic drawn as pixel position vs. supply voltage

In the end, the accumulated numerical data is saved in CSV format in order to be processed by other means. This type of data is easily interpreted by a variety of programs, such as spreadsheet calculus Fig. 25.

Clipboard Font

C3 560.011519

	A	B	C	D	E	F
1	Voltage [V]	LASER H [px]	LASER V [px]	Grid 1 H (px)	Grid 1 V (px)	Grid 2 H (px)
2	0	992.736419	559.113317	537.567666	43.797318	521.750664
3	1	992.804188	560.011519	537.624678	43.829105	521.725815
4	2	992.813757	559.445102	537.53112	43.843008	521.748679
5	3	992.626009	558.733322	537.512109	43.883116	521.695767
6	4	992.624251	558.016188	537.554064	43.798029	521.749987
7	5	992.685386	557.3685	537.479692	43.83401	521.693561
8	6	992.800929	556.510626	537.545879	43.854409	521.7036
9	7	992.988072	555.725065	537.496064	43.870297	521.753876
10	8	993.036138	554.722942	537.541388	43.863848	521.70415

Figure 25: Selection of saved numerical data fields

C) Data processing (converting pixels into milimeters)

Based on the data obtained from optical measurements it has been processed in Excel for the detected markers positions and LASER trace measured for the bidirectional LASER beam guidance system with bimorph actuators, this chart being presented in Fig. 26.

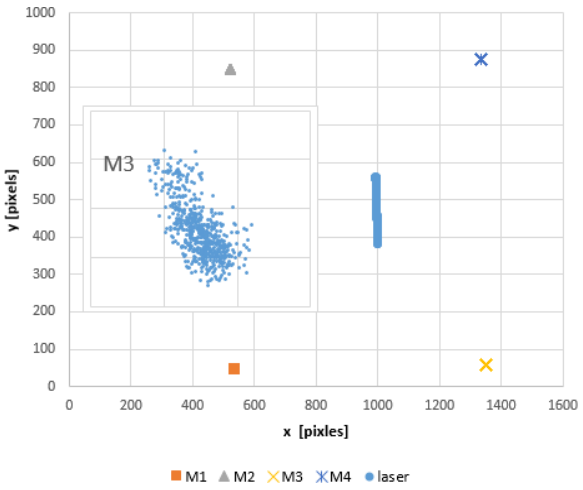

Figure 26: Detected markers positions and LASER trace. Zoomed in, the scatter of marker M3 position

Figure 26 shows the superposition of the dectect centers for markers and LASER spot. The detected center of the markers varies for each measurement point within 0.5 pixels. For each point, pixel postition of the LASER spot was converted to milimiters using its respective markers positions.

The displacement of the laser spot relative to its position at 0 V excitation is prezented in Fig. 27. The blue curve coresponds to the increasing voltage, while the orange coresponds to the decreasing voltage.

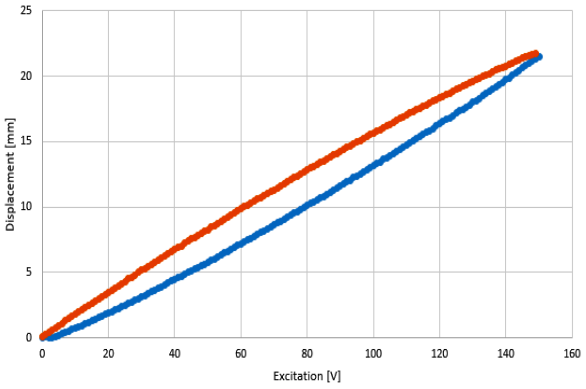

Figure 27: Measured histeresys curve for the piezo actuator type PB4VB2W

The presented histeresys curve in Fig. 27 is an average of two sets of measurements.

6. Conclusions

The paperwork is focused on testing the system which, to compensate for the tremor, uses an optical system for deflecting a LASER beam in two directions perpendicular to each other (X, Y), using two bimorphic piezoelectric actuators.

Starting from the presented constructive solution, a test stand was created which includes a deflection system with two bimorphic piezoelectric actuators, a LASER system, a voltage generator for the actuators and a webcam.

The characterization of the bimorphic actuators was performed by plotting the response curve, for displacements between 0 and 150 V. It was observed that it is preferable to fix the mirrors by gluing with adhesive directly on the surface of the bimorphic actuators.

A new method for determining the response curve has also been developed, using optical image capture and processing.

Comparing the results obtained by this method with those obtained by manual reading and measurement, it is found that similar results were obtained, relative to the type and maximum deflection of the tested actuators, which validates the new optical developed method.

In order to improve the research conducted, a primary evaluation of the potential sources of errors measurement, indicates that the most important step is to design an improved a test stand to provide better alignment of objects and possibilities to compensate for positioning errors.

The next step would be the development of parallax error and fisheye distortion compensation algorithms. Next in order would be the identification of a suitable uniform density distribution screen that would not alter the intensity of the light passing through and not induce errors in the calculation of center of mass of the relevant points.

There are several potential uncertainty sources for errors:

1. camera related:

1.1. possible dead pixels – an evaluation of the camera response was made and no dead pixels were found in this case,

1.2. fisheye or pincushion distortions – several grids were used and no such distortions were apparent to the naked eye but a numerical determination has to be done in the future to ensure the presence of such an algorithm,

1.3. imperfect focusing – this was an issue, the autofocusing algorithm of the camera being unreliable and focusing outside of the target screen,

2. screen related:

2.1. screen transmittance variability – the screen used was regular printing paper and light passing through presented islands of brightness,

2.2. grid printing errors – the only measurement method presently available is the use of a precision caliper and no significant errors were found,

3. test stand related:

3.1. parallax error between LASER deflection system and screen – there is such an error and it can be compensated or minimized by moving the stand on the table of an CMM type XOrbit 87 in order to check and adjust the position and orientation of the devices,

3.2. parallax error between camera and screen – same comments as for previous error,

3.3. variable illumination of screen due to light bulb flicker or various surfaces shining – it can cause some of the focusing errors and cause areas of local saturation but this can be filtered out of the analyzed image.

Acknowledgements

The authors acknowledge UEFISCDI for the support offered through the 20 PTE/2020 research grant – Sistem de compensare a vibraţiilor echipamentelor cu fascicul laser pentru microchirurgie (Vibration compensation system of laser beam equipment for microsurgery), which made this research possible, also this work was supported by the Romanian Ministry of Education, Research and Digitalization, project number 25PFE/30.12.2021 – Increasing R-D-I capacity for electrical engineering-specific materials and equipment with reference to electromobility and "green" technologies within PNCDI III, Programme 1.

References

[1] Comeagă, C.D., Grecu, E. - Control of Piezoelectric Actuators to Diminish the Influence of the Nonlinearity and Hysterezis, 5th Franco-Japanese Congress, October 9-11, Becancon – France, pp. 372-376, 2001.

[2] Alexandrescu, N ; Udrea, C ; Comeaga, D ; Ovezea, D ; Apostolescu, TC - Piezo-Electrically operated mini robot; IEEE International Conference on Automation, Quality and Testing, Robotics (AQTR), Cluj Napoca, May 22-25, 2008, Theta 16Th Edition, vol.II, Proceeding, Pages:392-397 ISBN:978-1-4244-2576-1.

[3] Alexandrescu N., Comeaga C.D. si colaboratorii, Realizarea de mini roboţi de înalta precizie, ctr. nr.38 CEEX-I 03/10.10.2005 din programul “Cercetare de excelenta”.

[4] J. N. Weiss, Treatment of central retinal vein occlusion by injection oftissue plasminogen activator into a retinal vein, Amer. J. Ophthalmol.,vol. 126, pp. 142–144, 1998

[5] R. A. MacLachlan, . C. Becker, J. Cuevas Tabar s, G. W. Podnar, L.A. Lobes, and C. N. Riviere, Micron: an actively stabilized handheld tool for

microsurgery, IEEE Trans Robot, vol. 28:1, pp.195-212, Feb.2012.
[6] K. M. Lee and D. K. Shah, Kinematic analysis of a three-degrees-offreedom in-parallel actuated manipulator, IEEE J. Robot. Autom., vol. 4,no. 3, pp. 354–360, Jun. 1988.
[7] B. Gonenc, P. Gehlbach, J. Handa, R. H. Taylor, and I. Iordachita, Motorized Force-Sensing Micro-Forceps with Tremor Cancelling and Controlled Micro-Vibrations for Easier Membrane Peeling, inProc. IEEE RAS EMBS Int. Conf. Biomed. Robot. Biomechatron.(BioRob'14), 2014, pp. 244-251.
[8] D. Y. Choi et al., Test of tracing performance with an active handheld micromanipulator, in Proc. 29th Annu. Int. Conf. IEEE Eng. Med. Biol. Soc., Aug. 2007, p. 3638-3641.
[9] I. Kuru, B. Gonenc, M. Balicki, J. Handa, P. Gehlbach, R. H. Taylor, and I. Iordachita, Force Sensing Micro-Forceps for Robot Assisted Retinal Surgery , in Proc. EMBC 2012, San Diego, CA, Aug 28-Sep 1, 2012, pp. 1401-1404.
[10] A. Üneri, M. a Balicki, J. Handa, P. Gehlbach, R. H. Taylor, and I. Iordachita, New steadyhand eye robot with micro-force sensing for vitreoretinal surgery, Proc. IEEE. RAS. EMBS. Int. Conf. Biomed. Robot. Biomechatron., vol. 2010, no. 26 29, pp. 814–819, Sep. 2010.
[11] M. Balicki, A. Uneri, I. Iordachita, J. Handa, P. Gehlbach, and R.Taylor, Micro-force sensing in robot assisted membrane peeling for vitreoretinal surgery, in Medical Image Computing and Computer-Assisted Intervention (MICCAI 2010) (T. Jiang, N. Navab, J. Pluim,and M. Viergever, eds.), vol. 6363 of Lecture Notes in Computer Science, pp. 303–310, Springer Berlin / Heidelberg, 2010.
[12] https://www.cedrat-technologies.com, accessed on: 07.02.2022.
[13] D. Ovezea et al., Piezoelectric Active Tremor Compensation System for LASER Microsurgery - Constructive Solution, 2021 12th international symposium on advanced topics in electrical engineering (ATEE), 2021, pp. 1-6, doi: 10.1109/ATEE52255.2021.9425130.
[14] https://www.thorlabs.com, accessed on: 07.02.2022.
[15] https://www.lasercomponents.com, accessed on: 07.02.2022.
[16] Emil-Ionut Nita, Edgar Moraru, Coanda Philip, Mircea Udrea, Experimental Setup for Static Characterization of Stack-Type Piezoelectric Actuators, in curs de publicare IJOMAM 2022.
[17] https://github.com/tedburke/RobotEyez, accessed on: 16.05.2022.